

Extracellular vesicles derived from melanoma cells induce carcinoma-associated fibroblasts via miR-92b-3p mediated downregulation of PTEN

Stefanie Kewitz-Hempel¹  | Nicola Windisch¹ | Gerd Hause² | Lutz Müller³ | Cord Sunderkötter¹ | Dennis Gerloff¹

¹Department of Dermatology and Venereology, Martin-Luther-University Halle-Wittenberg, Halle (Saale), Germany

²Biocenter, Martin-Luther-University Halle-Wittenberg, Halle (Saale), Germany

³Department of Internal Medicine IV, Hematology and Oncology, Martin-Luther-University Halle-Wittenberg, Halle (Saale), Germany

Correspondence

Dennis Gerloff, Department of Dermatology and Venereology, Martin-Luther-University Halle-Wittenberg, Halle (Saale), Germany. Email: dennis.gerloff@uk-halle.de

Funding information

Open Access Publishing by the German Research Foundation (DFG); Wilhelm Roux Funding Program by the medical faculty of the Martin-Luther-University Halle-Wittenberg

Abstract

In melanoma, carcinoma-associated fibroblasts (CAFs) are important cellular components in the tumour microenvironment due to their potential to promote tumour growth and metastatic spread of malignant cells. Melanoma cells have the ability to affect non-tumour cells in the microenvironment by releasing extracellular vesicles (EVs). The mechanisms responsible for reprogramming normal dermal fibroblasts (NHDFs) into CAFs remain incompletely understood. However, it is likely thought to be mediated by melanoma-specific miRNAs, which are transported by EVs derived from melanoma cells. Therefore, we wondered if one of the most enriched miRNAs in EVs secreted by melanoma cells, miR-92b-3p, is involved in the conversion of normal fibroblasts into CAFs. We observed that melanoma cell-derived EVs indeed delivered miR-92b-3p into NHDFs and that its accumulation correlated with CAF formation, as demonstrated by enhanced expression of CAF marker genes and increased proliferation and migration. Overexpression of miR-92b-3p in NHDFs revealed similar results, while EVs deficient of miR-92b-3p did not induce a CAF phenotype. As a target we identified PTEN, whose repression led to increased expression of CAF markers. We thus provide a novel pathway of intercellular communication by which melanoma cells control the transformation of CAFs by virtue of EV-transported miRNAs.

KEYWORDS

carcinoma-associated fibroblasts, extracellular vesicles, melanoma, miRNA

1 | INTRODUCTION

Malignant melanoma is a highly aggressive tumour with an increasing incidence and it accounts for the majority of skin cancer deaths (Friedrich & Kraywinkel, 2018). In tumorigenesis as well as tumour progression and metastasis, the tumour microenvironment (TME) is of particular importance in melanoma, mostly because it is the site of the immune response. It is composed of immune cells infiltrating the tumour (such as macrophages, granulocytes and T cells) as well as of non-immune cells from, for example, the surrounding connective tissue such as stromal cells (fibroblasts) and endothelial cells (Dehne et al., 2017; Hanahan & Coussens, 2012; Sunderkötter et al., 1994; Whiteside, 2008).

Carcinoma-associated fibroblasts (CAFs) represent activated fibroblasts of mesenchymal lineage in the TME of solid cancers with altered morphology and functions compared to normal fibroblasts. Their main function is the maintenance and remodelling

This is an open access article under the terms of the [Creative Commons Attribution-NonCommercial-NoDerivs License](https://creativecommons.org/licenses/by-nc-nd/4.0/), which permits use and distribution in any medium, provided the original work is properly cited, the use is non-commercial and no modifications or adaptations are made.

© 2024 The Authors. *Journal of Extracellular Vesicles* published by Wiley Periodicals, LLC on behalf of the International Society for Extracellular Vesicles.

of the extracellular matrix (ECM) mostly by the release of matrix metalloproteinases (MMPs) (Erdogan & Webb, 2017). Moreover, CAFs promote tumour growth and facilitate metastasis by promoting angiogenesis through the secretion of growth factors and cytokines (De Boeck et al., 2013; Shiga et al., 2015; Zhou et al., 2015). Furthermore, CAFs contribute to an immunosuppressive environment and limit antitumour immunity (Kalluri, 2016; LeBleu & Kalluri, 2018). In the context of melanoma, research findings indicate that CAFs present in the TME were associated with resistance against anti-PD-1 immunotherapy (Galbo et al., 2021). In vitro, CAFs have been shown to promote melanoma growth by increased expression of MMPs as well as IL-6 and IL-8 (Papaccio et al., 2021). Additionally, drug resistance of melanoma cells was increased when they were cultured on a CAF monolayer (Flach et al., 2011). While there is no unique classification for CAFs (Biffi & Tuveson, 2021; Davidson et al., 2020; Kanzaki & Pietras, 2020; Wu et al., 2021) they are generally defined through certain morphological changes (they are larger than resting fibroblasts, often with indented nuclei and branching cytoplasm), increased expression of α SMA, FAP, IL-6 as well as IL-8 and enhanced proliferation and migration (Glabman et al., 2022; Mazurkiewicz et al., 2022; Ping et al., 2021; Strnadova et al., 2022; Wang, Uemura et al., 2020; Wang, Fang et al., 2018; Wu et al., 2021).

It is known that melanoma cells contribute to the formation of CAFs. However, the mechanisms of reprogramming normal dermal fibroblasts into CAFs are not yet fully understood, but it is likely mediated by paracrine factors, cell-cell interactions and extracellular vesicles (EVs) that are secreted by cancer cells (Hu & Hu, 2019; Koyama et al., 2008; Romano et al., 2021; Shu et al., 2018). In analogy as demonstrated for tumour-associated macrophages (TAMs) as shown by our group (Gerloff et al., 2020) and others (Bardi et al., 2018; Marton et al., 2012).

EVs are cell-derived nanoparticles that are lipid-membrane bound and secreted by all cells during physiological and pathological states (Doyle & Wang, 2019; Mir & Goettsch, 2020). Their secretion is increased in malignant cells and their cargo differs between normal and cancer cells (Bebelmann et al., 2021; Gerloff et al., 2020, 2022). EVs are categorized based on size and biogenesis into three major subtypes: exosomes, microvesicles and apoptotic bodies (Doyle & Wang, 2019; Mir & Goettsch, 2020). Exosomes, originating from the endosomal compartment, are small (50–200 nm) lipid vesicles. They are created in multivesicular bodies (MVB) and discharged into the extracellular space through fusion with the cell membrane (Doyle & Wang, 2019; Mir & Goettsch, 2020; Yanez-Mo et al., 2015; Zaborowski et al., 2015). In contrast, microvesicles are larger in size (100–1000 nm) and are released into the extracellular environment by budding (shedding) or fission of the plasma membrane (Borges et al., 2013; Doyle & Wang, 2019; Mir & Goettsch, 2020; Zaborowski et al., 2015). Exosomes and microvesicles have in common that they shuttle a package of different functional biological molecules such as proteins, DNAs and RNAs (coding and non-coding RNAs like miRNAs) between different cells (Raposo & Stoorvogel, 2013; Xiao et al., 2012). They are especially relevant for the latter which would otherwise be degraded in the extracellular space.

Apoptotic bodies are the largest extracellular vesicles (1000–2000 nm). They are released during the disassembly of dying cells. Due to their size, apoptotic bodies contain higher quantities of lipids, proteins and nucleic acids. They include cellular components such as parts of cytosol, micronuclei or intact organelles. Apoptotic bodies are not known for their participation in intercellular communication; instead, they are assimilated and eliminated by phagocytic cells, such as macrophages (Borges et al., 2013; Doyle & Wang, 2019; Mir & Goettsch, 2020; Zaborowski et al., 2015).

While the cargo of apoptotic bodies is stochastic, the loading of small EVs (exosomes and small microvesicles) is an active, regulated process (Villarroya-Beltri et al., 2013). This was further supported by our previous analyses, which revealed significant differences in miRNA loading between EVs derived from melanoma cells and normal human epidermal melanocytes (NHEMs) and their cells from which they were secreted (Gerloff et al., 2020, 2022).

MiRNAs, which are small non-coding RNA molecules of approximately 22 nucleotides in length, are capable of post-transcriptionally regulating a variety of genes. Functional miRNAs are formed by two processing steps (pri-miRNA and pre-miRNA). The mature miRNA is then loaded into the RNA-induced silencing complex (RISC), which guides it to a complementary binding site in the 3' untranslated region (3'UTR) of a target RNA. Binding of the miRNA-RISC complex to this mRNA seeding sequence results in inhibition of protein translation or in increased degradation of transcript (Ambros, 2004; Bartel, 2004). Since miRNA-mRNA binding only needs to be partially complementary, a single miRNA can potentially have an effect on several mRNAs. In addition to this versatility, mRNAs usually have several potential binding sites for different miRNAs in their 3'UTR, thus several miRNAs have the potential to regulate the protein expression of a gene and act synergistically.

We have previously demonstrated that the transport of miR-125b-5p by melanoma cell-derived EVs induces a marked change in macrophage gene expression, resulting in a pro-tumorigenic phenotype (Gerloff et al., 2020).

In the context of CAFs, studies from other groups revealed that EVs derived from melanoma cell lines contribute to the formation of CAFs, for example, by the transport of miR-155-5p (Zhou, Yan, et al., 2018), miR-21 (Wang, Wang et al., 2020), and miR-210 (Shu et al., 2018). Dror et al. (2016) showed that the transport of miR-211 from early melanoma cells into fibroblasts induces formation of CAFs through the suppression of IGF2R (Dror et al., 2016), albeit this miRNA was shuttled not by EV, but by melanosomes, cell organelles specialized for pigment formation and distribution. Their study also demonstrated in vitro and in a murine melanoma model the tumour-promoting properties of the induced CAFs (Dror et al., 2016).

However, we did not find an enrichment of these miRNAs in melanoma cell-derived EVs. Instead, we found that miR-92b-3p is one of the most abundant and the highest enriched miRNA in EVs derived from melanoma cells compared to NHEM-derived EVs and we found miR-92b-3p significantly enriched in EVs obtained from the blood of melanoma patients (Gerloff et al., 2022).

Since miR-92b-3p targets PTEN directly in small cell lung cancer cells (Li et al., 2021) and since repression of PTEN leads to activation of the PI3K/AKT pathway, which is an important step in CAF formation (Wu et al., 2021), we wondered whether EV-mediated transport of miR-92b-3p from melanoma cells is involved in the conversion of normal fibroblasts into CAFs.

2 | MATERIALS AND METHODS

2.1 | Cell cultures

Melanoma cell lines (BLM and MV3) were cultured in DMEM (Gibco, Thermo Fisher Scientific, Waltham, Massachusetts, USA) supplemented with 10% foetal calve serum (FCS) (Sigma Aldrich, Taufkirchen, Germany) and 1% penicillin-streptomycin (Sigma Aldrich, Taufkirchen, Germany). Melanoma cell lines were provided from the Department of Dermatology, University of Münster, Germany. Primary normal human dermal fibroblasts (NHDFs) were isolated in our laboratory from juvenile foreskins of a total of 10 individual donors and cultured in fibroblast growth medium supplemented with basic fibroblast growth factor and insulin (all PromoCell, Heidelberg, Germany) as well as 1% penicillin-streptomycin. To account for inter-individual heterogeneity, all experiments were performed with NHDFs from at least three different donors. Primary normal human epidermal melanocytes (NHEM) were isolated in our laboratory from juvenile foreskins and cultured in medium 254 (Thermo Fisher Scientific, Waltham, Massachusetts, USA) including human melanocyte growth supplement (HMGS) and 1% penicillin-streptomycin. All cells were incubated at 37°C and 5% CO₂.

2.2 | Isolation and analysis of small extracellular vesicles

EVs were isolated and characterized according to the 2018 consensus statement on minimal information for studies of extracellular vesicles (MISEV2018) (Van Hove & Hoste, 2022). Cells were cultured for 48 h in DMEM supplemented with 10% exosome depleted FCS (Thermo Fisher Scientific, Waltham, Massachusetts, USA) and 1% penicillin-streptomycin. Supernatants (30 mL) were collected and centrifuged for 10 min at 300 × g to remove cells and cell debris, followed by 30 min at 10,000 × g to remove larger vesicles. Afterwards the supernatants were filtered through a 0.2 µm filter and centrifuged at 100,000 × g for 2 h. Centrifugation was performed using a Sorvall WX+ Ultra Centrifuge, with SureSpin 632 rotor (k-factor 194) (Thermo Fisher Scientific, Waltham, Massachusetts, USA). EVs were resuspended in PBS and size-exclusion chromatography was performed according to the manufacturer's protocol (Cell Guidance Systems, Cambridge, UK). EV analysis was performed by nanoparticle tracking analysis (NTA) using a NanoSight NS300 (Malvern Panalytical, Kassel, Germany). Therefore, EVs were isolated and analysed from three independent biological samples. Measurements were performed at a controlled temperature of 22°C. For each sample, three measurements of 30 s were performed. EV concentration and size was calculated by the NanoSight software.

2.3 | Transmission electron microscopy (TEM)

To prepare TEM-samples 3 µL of the dispersion were spread onto Cu-grids coated with a formvarfilm. After 1 min of adsorption, excess liquid was blotted off with filter paper. Subsequently the grids were air-dried for 15 s, washed with water (three times for 1 min), placed on a droplet of 2% aqueous uranyl acetate and drained off after 1 min. The dried specimens were examined with an EM 900 transmission electron microscope (Carl Zeiss Microscopy, Jena, Germany) at an acceleration voltage of 80 kV. Electron micrographs were taken with a Variosped SSCCD camera SM-1k-120 (TRS, Moorenweis, Germany).

2.4 | Immunoblot analyses

Cells and EVs were lysed by RIPA buffer for 30 min at 4°C. About 20 µg of protein extracts were resolved by SDS-PAGE and blotted to nitrocellulose membranes and probed with the following antibodies: anti-CD81 (5A6) (1:200); anti-CD63 (MX-49.129.5) (1:500); anti-ALIX (1A4) (1:250); anti-CANX (AF18) (1:500); anti-PTEN (A2B1) (1:500); anti-GAPDH (0411) (1:1000); anti-αSMA(1A4) (1:200) (all Santa Cruz, Dallas, USA), anti-CD9 (CGS12A) (1:1000) (Cell Guidance Systems, Cambridge, UK) and anti-Phospho-p44/42 MAPK (Erk1/2) (Thr202/Tyr204) (197G2), anti-Phospho-Akt (Ser473) (D9E) XP, anti-p44/42 MAPK (Erk1/2) (137F5), anti-Akt (11E7), anti-Vimentin (D21H3), anti-p16 INK4A (D3W8G), anti-21 Waf1/Cip1 (12D1), anti-PDGF Receptor α (D1E1E) XP (all Cell Signalling Technology, Leiden, Netherlands). Antibody incubation was performed in 5% milk or 5% BSA at 4°C over night. For antibody detection, blots were incubated for 1 h at room temperature with m-IgGκ BP-HRP (1:5000) (Santa Cruz, Dallas, USA) or anti-mouse IgG-HRP (1:2000) (Cell Signalling Technology, Leiden, Netherlands). Chemi-

luminescent detection was performed using Amersham ECL Prime (GE Healthcare, Amersham, UK). Fold change of protein levels were calculated by Fiji software (Schindelin et al., 2012).

2.5 | β -Galactosidase staining

NHDFs were cultured for 24 h with indicated treatments, followed by β -galactosidase staining, which was performed with the Senescence β -Galactosidase Staining Kit (Cell Signalling Technology, Leiden, Netherlands) according to the manufacturer's instructions.

2.6 | ELISA

Measurement of IL-6 and IL-8 secretion was performed by ELISA. NHDFs were cultured for 24 h with indicated treatments. Afterwards, ELISA was performed by IL-6 Human ELISA KIT and IL-8 Human ELISA KIT (Thermo Fisher Scientific, Waltham, Massachusetts, USA) according to the manufacturer's instructions.

2.7 | RNA isolation and analyses

Total RNA was extracted from cells or EVs using TriFast™ reagent (Qiagen, Erlangen, Germany), according manufacturer's protocol. RNA quality and quantity was analysed by Agilent bioanalyser (Agilent, Santa Clara, California, USA). MiRNA quantification was performed by qRT-PCR using TaqMan® MicroRNA Reverse Transcription Kit and TaqMan® Universal Master Mix II according manufacturer's instructions (Thermo Fisher Scientific, Waltham, Massachusetts, USA). Values were normalized by RNU6 for cells, while for EV values were normalized by miR-16, because it was highly and stably expressed in our NGS analysis and it was earlier reported as endogenous normalization miRNA in exosomes (Lange et al., 2017). Relative fold changes were calculated by $2^{-\Delta\Delta C_t}$ method (Livak & Schmittgen, 2001), comparing the values to the mean of the control group. MiRNA assays were purchased from Thermo Fisher Scientific (Thermo Fisher Scientific, Waltham, Massachusetts, USA).

2.8 | Transcriptional analysis by qRT-PCR

The total RNA was isolated using TriFast™ reagent (Qiagen). For quantitative RT-PCR we used PowerUp™ SYBR™ Green master mix (Thermo Fisher Scientific) following the manufacturer's instructions. qPCRs were performed on QuantStudio™ 5 Real-Time PCR Systems. For normalization we used GAPDH. The following primers were used:

GAPDH for	ACCACAGTCCATGCCATCAC
GAPDH rev	TCCACCACCCTGTTGCTGTA
FAP for	CAAAGGCTGGAGCTAAGAATCC
FAP rev	ACTGCAAACATACTCGTTTCATCA
IL6 for	GACAGCCACTCACCTCTTCAGA
IL6 rev	GTGCCTCTTTGCTGCTTTCAC
IL8 for	GCTAAAGAACTTCGATGTCAGTGC
IL8 rev	CTCAGCCCTCTTCAAAACTTCTC

2.9 | Transfections

miR-92b-3p mimic, control mimic, Long nucleic acid (LNA)-92b-3p, LNA-control, PTEN siRNA and control siRNA were purchased by Qiagen (Hilden, Germany). Cells were transfected with 100 nM mimics, LNA or siRNA using Lipofectamine 3000 reagent (Invitrogen) following the manufacturer's instructions.

2.10 | BrdU assay

Cell proliferation was measured using BrdU Assay (Roche, Merck, Darmstadt, Germany) according to manufacture protocol. For indirect co-culture experiments melanoma cells were exposed to pre-treated fibroblasts for 24 h.

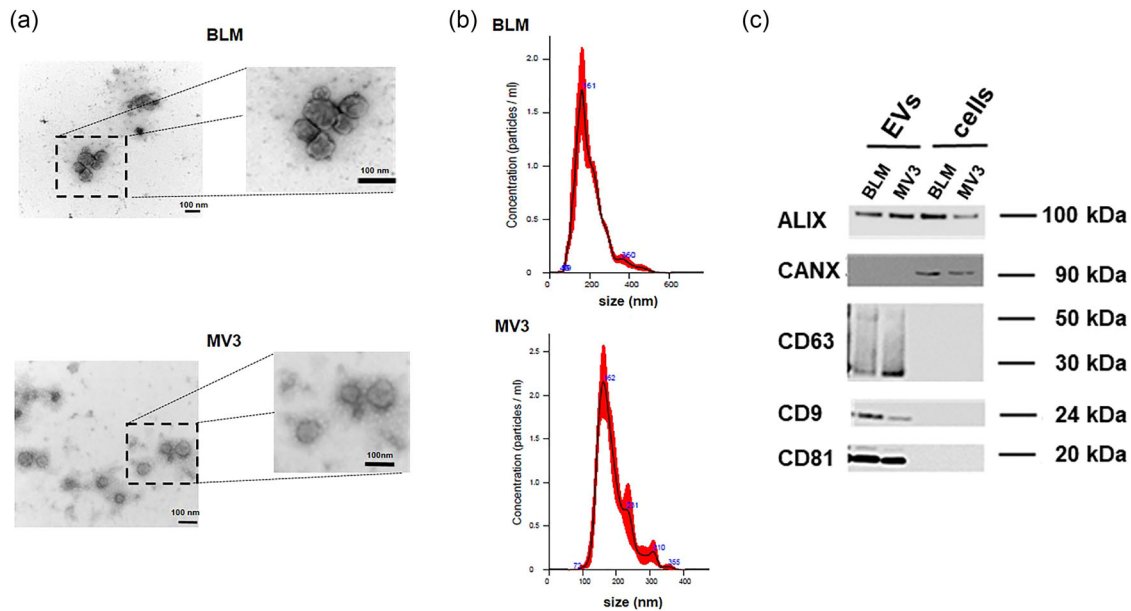


FIGURE 1 Characterization of extracellular vesicles derived from BLM and MV3. (a) TEM studies of EVs isolated from cell culture supernatants. The size scale corresponds to 100 nm. (b) Measurement of particle concentration or particle size of isolated EVs by nanoparticle tracking analysis (NTA). (c) Western blot analysis of EVs and corresponding cells analysed for CD63, CD81, CD9, ALIX and CANX.

2.11 | Wound closure assay

NHDFs or melanoma cell lines (MV3) were seeded in 12-well plates. Once the cells were confluent, a gap was manually drawn in the cell monolayer with a plastic pipette tip. The width of the wound was measured at several sites after 0, 6 and 24 h using a Mica microscope (Leica). For indirect co-culture experiments melanoma cells were exposed to pre-treated fibroblasts for indicated time.

2.12 | Cell fixation, staining and microscopic analysis

NHDFs were fixed with 4% paraformaldehyde for 20 min, after a washing step with PBS, fixed cells were incubated with 0.1% Triton X 100 for 15 min. Staining was performed, after washing with PBS, with Phalloidin and DAPI. Images were obtained using MIKA fluorescence microscope.

2.13 | Graphs and statistics

For the statistical analyses and graphical representation Graph Pad Prism software was used. To prove the statistical significands of the data, two tailed Student's *t*-test or Mann–Whitney *U*-test was performed, depending on Gaussian distribution, which was evaluated by the Levene test. A *p*-value ≤ 0.05 was considered as statistical significant.

Single cell RNA sequencing data (GSE254918) were obtained from Gene Expression Omnibus (GEO) (www.ncbi.nlm.nih.gov/geo).

3 | RESULTS

3.1 | Isolation and characterization of extracellular vesicles (EVs) derived from melanoma cell lines

TEM studies of EVs derived from the melanoma cell lines BLM and MV3 reveal a distinct vesicle structure with characteristic ultrastructure corresponding to the size of approximately 50–200 nm determined by NTA (Figure 1a,b). Western blot detects the classical EV surface proteins CD9, CD63 and CD81 (all tetraspanins), as well as the cytosolic protein ALIX. In contrast, CANX, an endoplasmic reticulum protein, serves as a control for cellular contaminants (Figure 1c).

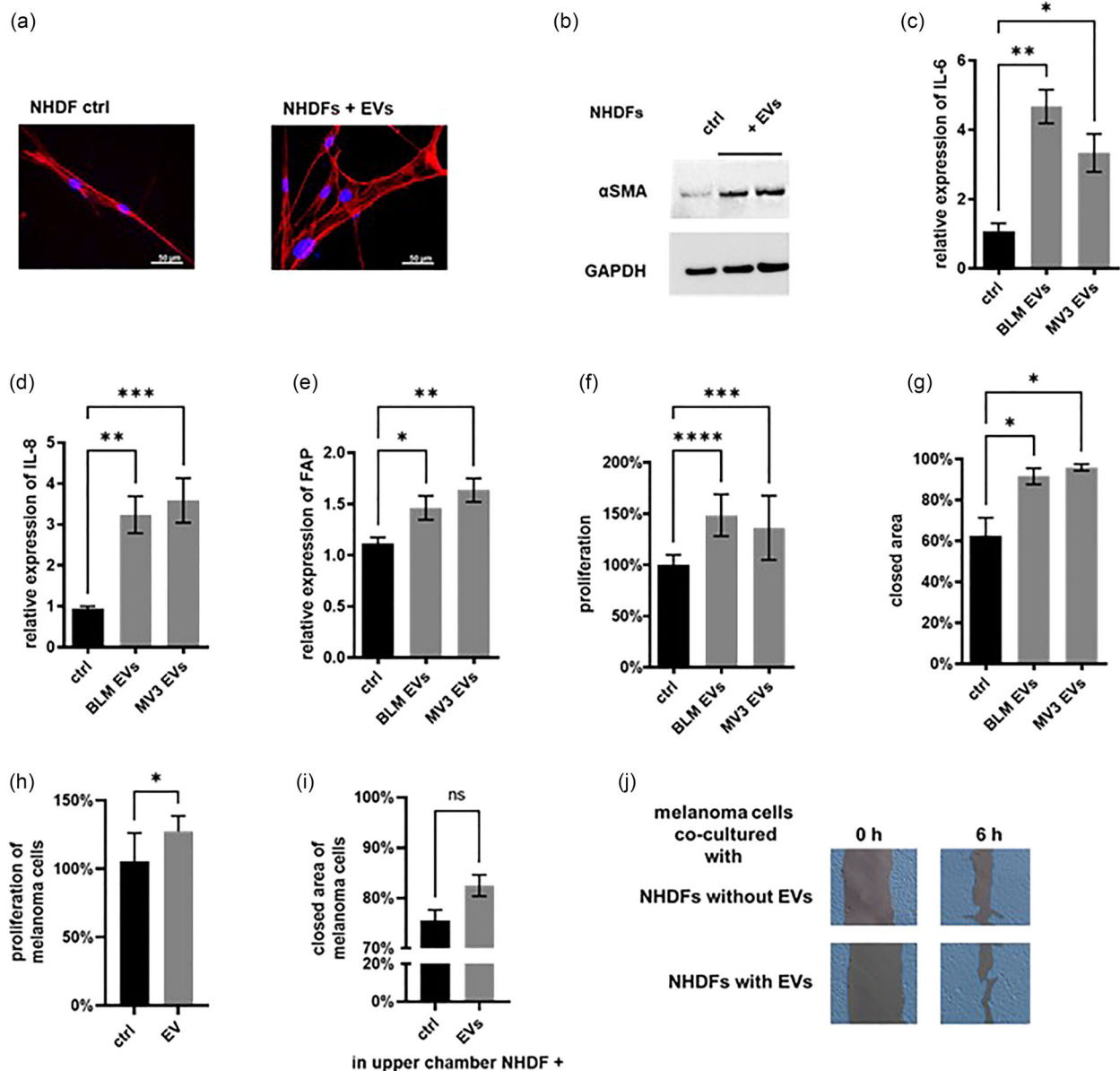


FIGURE 2 Melanoma cell-derived EVs induce a CAF phenotype in normal human dermal fibroblasts (NHDFs). NHDFs were incubated with or without melanoma cell-derived EVs (10 $\mu\text{g}/\text{mL}$ BLM and MV3) for 48 h and the resulting phenotype was analysed. (a) Representative images of actin filament staining (red) with Alexa FluorTM 594 phalloidin and nuclei staining with DAPI (blue) (scale bar represents 50 μm). CAF marker genes were analysed by (b) Western blot for αSMA and qRT-PCRs for (c) IL-6, (d) IL-8 and (e) FAP. In addition, (f) proliferation and (g) migration of MV3 co-cultured with NHDFs pre-incubated with (10 $\mu\text{g}/\text{mL}$) or without MV3-derived EVs. (h) Proliferation and (i/j) migration of MV3 co-cultured with NHDFs pre-incubated with (10 $\mu\text{g}/\text{mL}$) or without MV3-derived EVs. (k) Representative images of the wound closure assay 6 h after the wound was inflicted. (Bars represent mean \pm standard deviation of at least three individual experiments on NHDFs from different donors; * $p \leq 0.05$; ** $p \leq 0.01$; *** $p \leq 0.001$; **** $p \leq 0.0001$; n.s., not significant).

3.2 | Melanoma cell-derived EVs induce a CAF phenotype in normal human dermal fibroblasts (NHDFs)

In order to investigate if melanoma cell-derived EVs induce CAF formation in primary normal human dermal fibroblasts (NHDFs) we incubated NHDFs with 10 $\mu\text{g}/\text{mL}$ EVs derived from melanoma cell lines BLM and MV3. EV-exposed NHDFs showed (i) a widespread shape with stress-contractile fibres (Figure 2a, Figure S1) and (ii) an increased expression of αSMA (Figure 2b) as well as IL-6, IL-8 and FAP (Figure 2c–e), which are widely used CAF marker genes (Augsten, 2014; Giusti et al., 2022; Hu & Hu, 2019; Kalluri & Zeisberg, 2006; Orimo & Weinberg, 2007; Tao et al., 2017), which we therefore limited to these in our further experiments. In addition, we found an increased expression of vimentin and PDGF receptor as well as an increase

in senescence markers such as p16, p21 and β -galactosidase activity in NHDFs after treatment with EVs derived from BLM or MV3 cells (Figure S2).

Our functional studies revealed increased proliferation (Figure 2f) and enhanced migration (Figure 2g) of NHDFs incubated with melanoma cell-derived EVs compared to control NHDFs. We observed only minor differences in CAF formation depending on the use of EVs derived from BLM or MV3 cells. Only for IL-6 expression, we observed a stronger induction in NHDFs incubated with EVs derived from BLM cells compared to those derived from MV3.

Indirect co-culture of melanoma cell lines with EV-induced CAFs reveal an increased proliferation and migration of melanoma cells (Figure 2h–j). These results demonstrated that treatment of NHDFs with EVs derived from melanoma cell lines induce tumour-promoting CAFs.

In summary, incubation of NHDFs with EVs derived from melanoma cell lines induces a CAF phenotype according to the commonly used definition and criteria, with tumorigenic properties.

3.3 | MiR-92b-3p accumulation in NHDFs induces CAF formation

Since miR-92b-3p is one of the most abundant and the highest enriched miRNA in melanoma cell-derived EVs in vitro (Figure S3) (Gerloff et al., 2022) and in vivo (EVs from melanoma patient serum) we analysed the enrichment of miR-92b-3p in NHDFs after incubation with 10 μ g/mL melanoma cell-derived EVs. We detected an accumulation of miR-92b-3p in NHDFs incubated with melanoma cell-derived EVs. In contrast, incubation with EVs derived from NHEMs showed no enrichment of miR-92b-3p (Figure 3a). These results suggest that miR-92b-3p is transported into NHDFs by melanoma cell-derived EVs.

To investigate whether miR-92b-3p contributes to EV-mediated reprogramming of normal fibroblasts into CAFs, we transfected NHDFs with 100 nM miR-92b-3p mimics (Figure 3b). In NHDFs overexpressing miR-92b-3p, we observed (i) widespread shaped fibroblasts and (ii) increased expression of CAF marker genes (α SMA, FAP, IL-6 and IL-8) (Figures 3c–g and S1), similar to NHDFs incubated with melanoma cell-derived EVs (Figure 2).

Furthermore, our functional assays showed that overexpression of miR-92b-3p induced proliferation and migration of NHDFs (Figure 3h,i).

In indirect co-culture of melanoma cells with miR-92b-3p-overexpressing NHDFs we also observed an increased migration and proliferation of melanoma cells (Figure 3j–l).

Prevention of miR-92b-3p incorporation into melanoma cell-derived EVs by locked nucleic acids (LNA) abolished EV-mediated induction of the CAF phenotype

To confirm that miR-92b-3p contributes to CAF formation, we inhibited the loading of miR-92b-3p into EVs by transfecting melanoma cells with 100 nM locked nucleic acids (LNA) against miR-92b-3p or a negative control and EVs were isolated from the supernatant (after 48 h). By qRT-PCR we confirmed a reduction of miR-92b-3p in EVs isolated from melanoma cell lines transfected with LNA-92b-3p (Figure 4a). As consequence, accumulation of miR-92b-3p in NHDFs incubated with these EVs was reduced in comparison to EVs derived from melanoma cells transfected with LNA control (Figure 4b). In NHDFs incubated with 10 μ g/mL EVs isolated from melanoma cell lines transfected with LNA-92b-3p we observed (i) spindle shaped fibroblasts (Figure 4c, Figure S1) and (ii) no or a reduced induction of CAF marker genes α SMA, IL-6, IL-8 and FAP (Figure 4d–g).

Furthermore, our functional assays showed a marginal enhancement in proliferation and migration for NHDFs incubated with EVs lacking miR-92b-3p cargo (Figure 4h,i).

Indirect co-culture of NHDFs that had previously been incubated with EVs devoid of miR-92b-3p cargo with melanoma cells did not lead to an enhancement of migration or proliferation of the melanoma cells (Figure 4j–l).

We were able to demonstrate the induction of CAFs through the overexpression of miR-92b-3p, whereas EVs lacking miR-92b-3p were not able to induce CAFs. We aimed to investigate the molecular mechanism by which miR-92b-3p contributes to CAF formation.

3.4 | MiR-92b-3p targets PTEN in NHDFs

To search for possible targets of miR-92b-3p, we used databases and identified the tumour suppressor PTEN (Figure 5a). Accordingly, treatment with melanoma cell-derived EVs or overexpression of miR-92b-3p leads to decreased expression of PTEN protein in NHDFs (Figure 5b,c). Reanalysis of a public available single cell RNA sequencing dataset (GSE254918) of in vivo fibroblast isolated from normal skin of healthy donors or from melanoma tumours revealed decreased expression of PTEN in melanoma tumour-associated fibroblasts (Figure 5d).

To prove that PTEN is a crucial factor in CAF generation we generated NHDF cells with 100 nM PTEN knockdown. To confirm PTEN knockdown in NHDFs by siRNA, Western blot analysis was performed (Figure 5e). The resulting knockdown led to (i) a widespread shape with stress-contractile fibres (Figures 5f and S1) and (ii) the upregulation of CAF markers IL-6, IL-8 and FAP (Figure 5g–i).

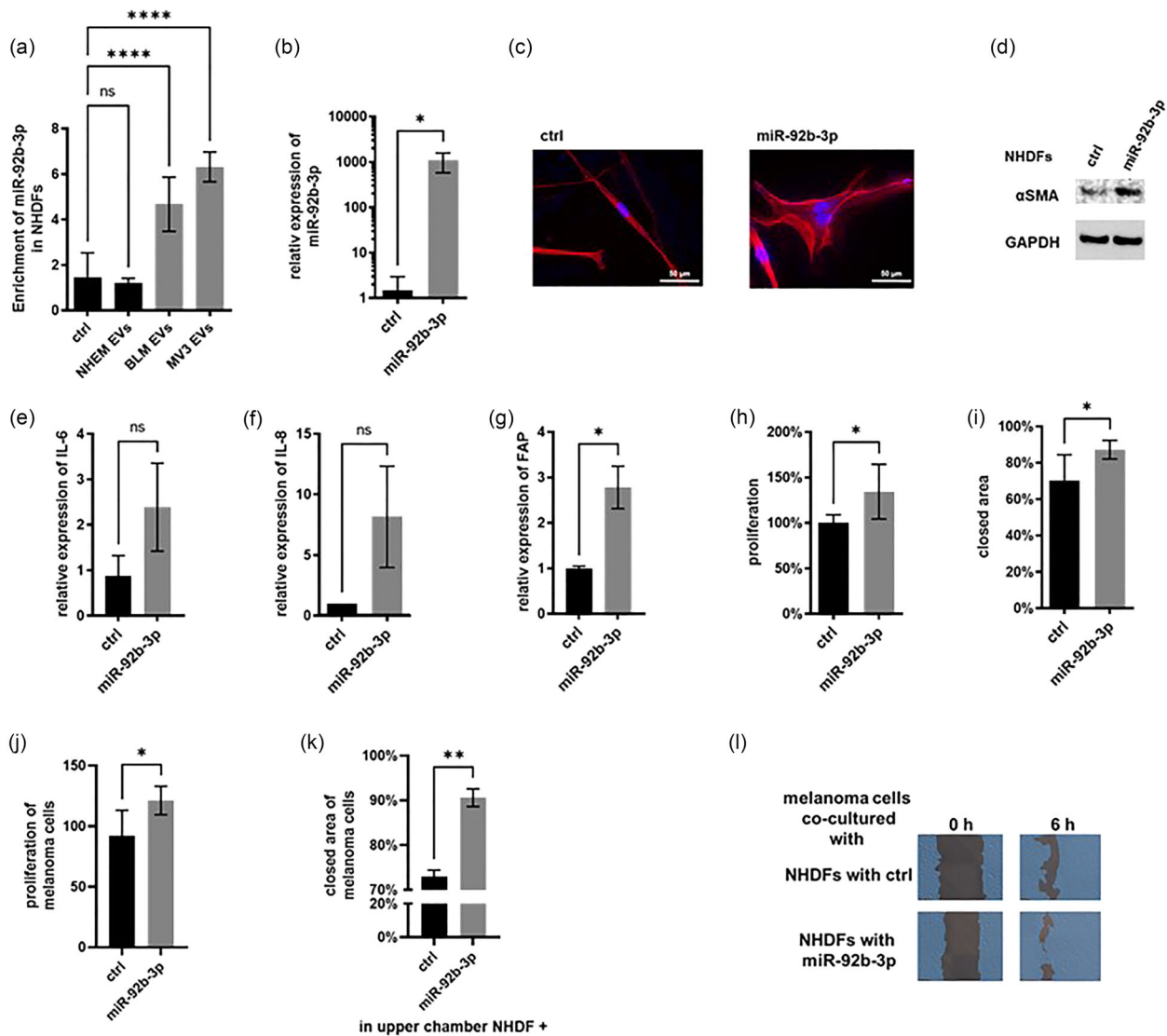


FIGURE 3 Overexpression of miR-92b-3p mimics CAF phenotype in NHDFs. (a) qRT-PCRs for miR-92b-3p in NHDFs after incubation with 10 µg/mL EVs derived from melanoma cells. EVs from NHEMs or normal medium were used as control. NHDFs were transfected with 100 nM miR-92b-3p mimic or control mimic (ctrl). The resulting phenotype was analysed 48 h after transfection. (b) qRT-PCRs to validate miR-92b-3p overexpression in NHDFs after transfection. (c) Representative images of actin filament staining (red) with Alexa Fluor™ 594 phalloidin and nuclei staining with DAPI (blue). The scale bar represents 50 µm. CAF marker genes were analysed by d) Western blot analysis for αSMA and qRT-PCRs for (e) IL-6, (f) IL-8 and (g) FAP. (h) Proliferation and (i) migration assays of NHDF cells transfected with miR-92b-3p mimic or control. (j) Proliferation and (k,l) migration of MV3 co-cultured with NHDFs transfected with 100 nM miR-92b-3p mimic or control. (l) Representative images of the wound closure assay 6 h after the wound was inflicted (Bars represent mean ± standard deviation of at least three individual experiments on NHDFs from different donors; * $p \leq 0.05$; ** $p \leq 0.01$; **** $p \leq 0.0001$; n.s., not significant).

In addition, our functional assays showed that NHDFs transfected with siPTEN showed increased migration (Figure 5j). Whereas no differences in proliferation were observed (data not shown).

To confirm that miR-92b-3p's PTEN inhibition leads to the tumour-promoting properties of NHDFs we also incubated melanoma cells with NHDFs transfected with siRNA against PTEN.

Similar to previous results obtained with EV-induced CAFs and miR-92b-3p overexpressing NHDFs, we observed increased proliferation and migration capabilities of melanoma cell lines (Figure 5k–m).

Since PTEN is involved in the regulation of PI3K/AKT and MAP kinase signalling, important pathways in CAF formation, we performed Western blot analyses to evaluate the phosphorylation status of AKT and ERK 1/2 in NHDFs during CAF formation induced by melanoma cell-derived EVs, miR-92b-3p overexpression or PTEN knockdown by siRNA. While ERK 1/2 phosphorylation shows no differences, we found an increase in AKT phosphorylation after overexpression of miR-92b-3p or siRNA-mediated knockdown of PTEN in NHDFs (Figure S4). This suggests, that miR-92b-3p mediated down regulation of PTEN contributes to CAF formation.

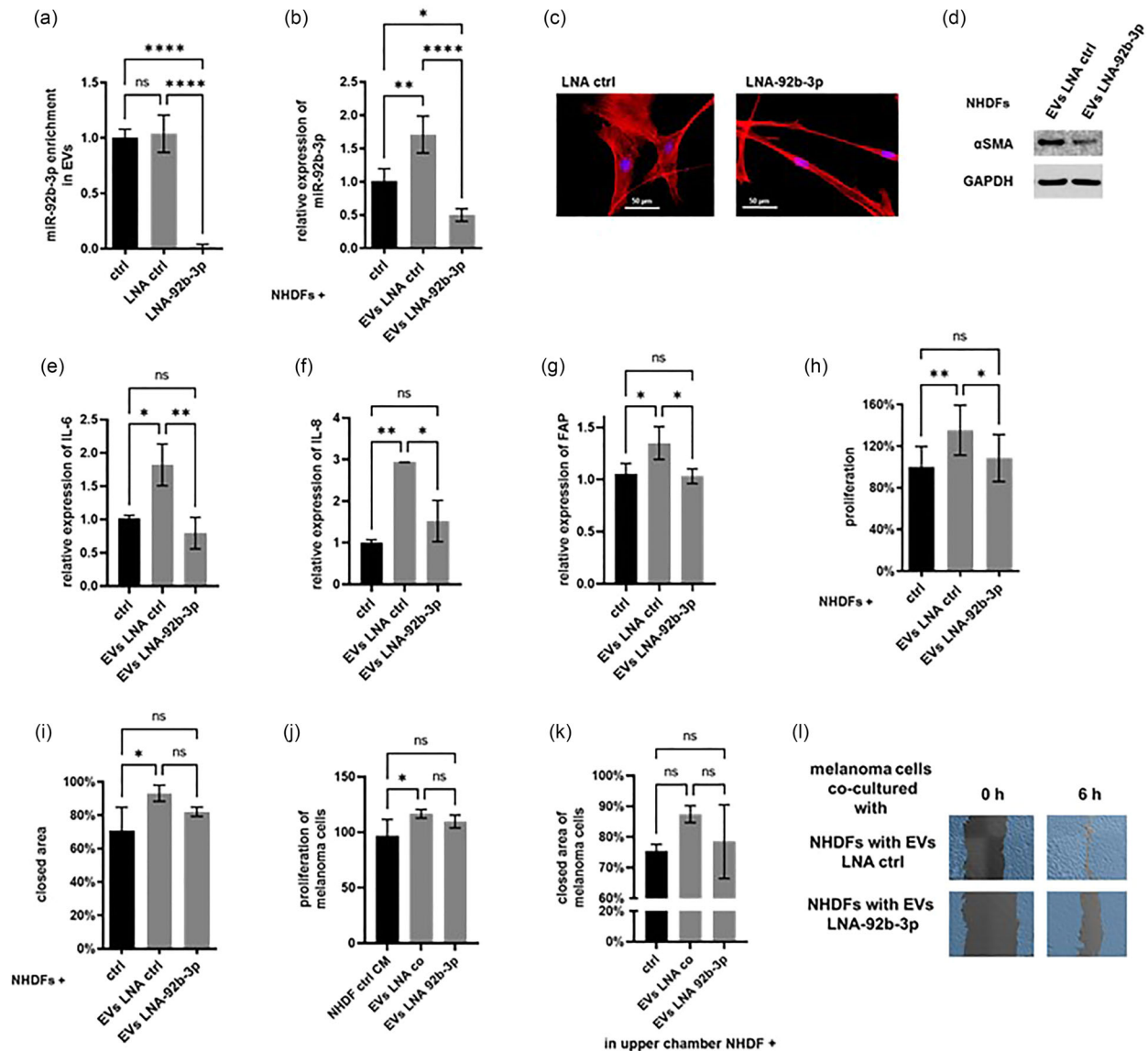


FIGURE 4 Locked nucleic acids (LNA) mediated miR-92b-3p inhibition prevents EV-induced CAF formation. Melanoma cells were transfected with 100 nM LNA-92b-3p or LNA ctrl. Non-transfected cells were used as control (ctrl). (a) 48 h after transfection, EVs were isolated and analysed by qRT-PCR for miR-92b-3p enrichment. NHDFs were incubated with or without the indicated EVs (10 μ g/mL) and analysed for (b) miR-92b-3p accumulation. (c) Representative images of actin filament staining (red) with Alexa Fluor™ 594 phalloidin and nuclei staining with DAPI (blue). The scale bar represents 50 μ m. CAF marker genes were analysed by (d) Western blot analysis for α SMA and qRT-PCRs for (e) IL-6, (f) IL-8 and (g) FAP. Functional assays examined (h) proliferation and (i) migration. (j) Proliferation and K/L migration of MV3 co-cultured with NHDFs pre-incubated with 10 μ g/mL EVs lacking miR-92b-3p cargo or control EVs. (k) Representative images of the wound closure assay 6 h after the wound was inflicted (Bars represent mean \pm standard deviation of at least three individual experiments on NHDFs from different donors; * $p \leq 0.05$; ** $p \leq 0.01$; *** $p \leq 0.001$).

4 | DISCUSSION

In this study, we have shown that the transport of miR-92b-3p by melanoma cell-derived EVs into normal fibroblasts contributes to CAF formation, by targeting PTEN. We provide evidence (1) that miR-92b-3p is enriched in melanoma cell-derived EVs, (2) that miR-92b-3p is transported into normal fibroblasts, (3) that enrichment of miR-92b-3p in fibroblasts induces markers and functional properties characteristic for CAF and 4) that knockdown of the miR-92b-3p target PTEN contributes to CAF formation.

The fact that melanoma cell-derived EVs mediate CAF formation had been shown only for fibroblast cell lines and characteristics of CAF were not always fully described (Hu & Hu, 2019; Shu et al., 2018; Zhou, Yan, et al. 2018; Wang, Wang, Uemura et al., 2020). We wanted to investigate the influence of melanoma cell-derived EVs on primary fibroblasts ex vivo. Therefore, we

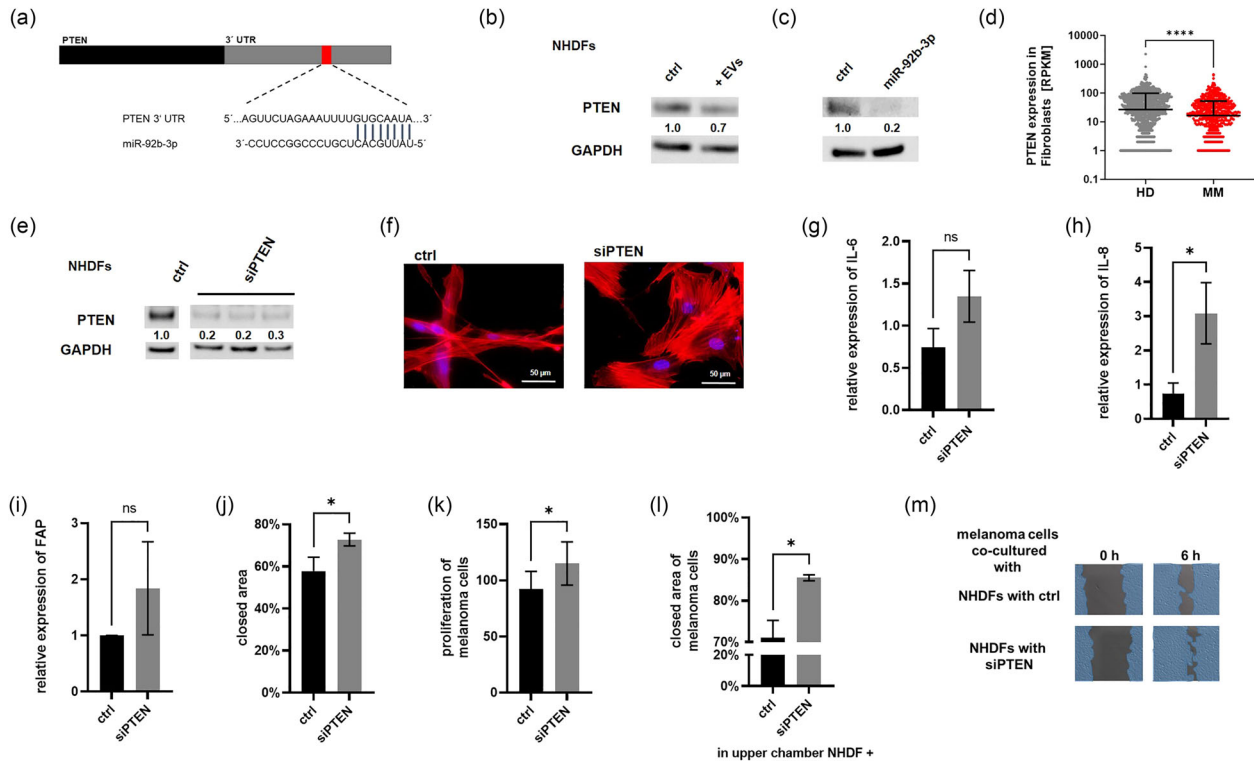


FIGURE 5 MiR-92b-3p targets PTEN in NHDFs. (a) Scheme of the predicted miR-92b-3p binding site in the PTEN 3'UTR. Western blot analysis for PTEN of (b) NHDFs incubated with 10 μ g/mL melanoma cell-derived EVs or without (ctrl) and (c) NHDFs transfected with 100 nM miR-92b-3p mimic or control mimic (ctrl). (d) Single cell sequencing analysis (GSE254918) of PTEN expression of in vivo Fibroblasts derived from normal skin of healthy donors (HD) or malignant melanoma tumours (MM). (e) Western blot analysis for PTEN of NHDFs transfected with 100 nM PTEN siRNA. (f) Representative images of actin filament staining (red) with Alexa Fluor™ 594 phalloidin and nuclei staining with DAPI (blue). (Scale bar represents 50 μ m). Analysis of CAF marker genes by qRT-PCR for (g) IL-6, (h) IL-8 and (i) FAP. (j) Functional assays examined migration. (k) Proliferation and (l) migration of MV3 co-cultured with NHDFs transfected with 100 nM PTEN siRNA or control. (m) Representative images of the wound closure assay 6 h after the wound was inflicted. (Bars represent mean \pm standard deviation of at least 3 individual experiments on NHDFs from different donors; **** $p \leq 0.0001$; * $p \leq 0.05$; n.s.: not significant).

apply a set of phenotypic and functional criteria for resulting CAFs. Isolation and characterisation of EVs used in our study was in accordance with MISEV 2018 guidelines (Théry et al., 2018).

From our previous investigations, we know that EV-delivered miRNAs have the ability to manipulate recipient cell phenotype (Gerloff et al., 2020), and that the miRNA load of melanoma cell-derived EVs differs from that of normal melanocytes (Gerloff et al., 2022).

Due to the significant increase of miR-92b-3p levels in both, several melanoma cell lines and their EVs compared to normal melanocytes and EVs derived from them (Gerloff et al., 2022), we focused our analysis on miR-92b-3p. We observed that EVs derived from melanoma cells transport miR-92b-3p into NHDFs and its accumulation correlates with CAF formation, as demonstrated by enhanced expression of CAF marker genes and increased proliferation and migration. Overexpression of miR-92b-3p in NHDFs shows similar results, while EVs lacking miR-92b-3p do not induce the CAF phenotype. The induction of CAF marker expression was comparable to previous studies investigating EV- or melanosome-mediated induction of CAFs in melanoma (Dror et al., 2016; Zhou, Yan, et al. 2018). EV-derived miRNAs have been shown to lead to formation of CAFs in other malignancies: The transport of miR-125b by EVs derived from human and mouse breast cancer cells promoted the differentiation of human normal foetal tissue fibroblasts into CAFs by targeting TP53INP1 (Vu et al., 2019). There are 2 studies on influence of miRNAs from melanoma cell-derived EVs on mouse fibroblasts. The delivery of miR-21 inhibited TIMP3, which resulted in an invasive CAF phenotype with increased expression of MMP2 and MMP9 (Wang, Wang et al., 2020). A second study focusses on miRNAs that target SOCS1 (which was downregulated during CAF formation) and identified miR-155-5p as a miRNA which was transported by EVs derived from melanoma cell lines in to fibroblasts where it lead to a pro-angiogenic switch of CAFs through activation of the JAK2/STAT3 pathway (Zhou, Yan, et al. 2018).

In addition, it has been reported that melanoma cells can also induce CAF formation through the melanosome mediated transport of miR-211 (Dror et al., 2016). However, in our analysis we did not find an enrichment of either miR-21, miR-155-5p or miR-211 in all EVs of various melanoma cell lines or in melanoma cells.

Instead, we had identified miR-92b-3p. This miRNA was higher expressed in primary melanomas compared to benign nevi (Dika et al., 2021). These results are consistent with our previous work that revealed an increased enrichment of miR-92b-3p in EVs derived from blood of melanoma patients in comparison to healthy donors (Gerloff et al., 2022).

MiR-92b-3p has been ascribed tumorigenic properties in malignancies before, but has never been related to the formation of CAFs. It had been shown that miR-92b-3p contributes to proliferation, migration, invasion in various types of cancers like glioblastoma (Xu et al., 2017), gastric cancer (Li et al., 2019), colorectal cancer (Gong et al., 2018), oesophageal squamous cell carcinoma (Wang et al., 2019), non-small cell lung cancer cells (Lei et al., 2014), clear cell renal cell carcinoma (Wang, Uemura, et al., 2020), as well as prostate cancer (Wang et al., 2021). With regard to tumour cell derived EVs miR-92b-3p was found to be enriched in small cell lung cancer (Li et al., 2021), synovial sarcoma (Uotani et al., 2017) and gastric cancer (Tang et al., 2020).

Since PTEN had been identified as a prominent target of miR-92b-3p in context of several malignancies (Li et al., 2021; Xu et al., 2017), we investigated the dependence of PTEN expression on miR-92b-3p in our system and found that both treatment of NHDFs with EVs from melanoma cells and overexpression of miR-92b-3p lead to a reduction in PTEN protein and induce CAF formation. Indeed, we found reduced PTEN expression during CAF formation in a public available in vivo dataset (GSE254978) comparing gene expression of fibroblasts in melanoma tumours to fibroblasts in healthy skin by single-cell RNA sequencing.

In glioblastoma (Xu et al., 2017) as well as in small cell lung cancer (Li et al., 2021) it was shown that miR-92b-3p mediated repression of PTEN induces the PI3K/AKT pathway. Consistently, we observed increased AKT phosphorylation following miR-92b-3p overexpression or siRNA-mediated PTEN knockdown in NHDFs (Figure S4). Since PTEN inhibits the PI3K/AKT/mTOR pathway, which is the main pathway of CAF differentiation (Li et al., 2021; Wu et al., 2021), we hypothesize that the observed suppression of PTEN contributes to the transformation of NHDFs into CAFs. As experimental proof of our hypothesis we demonstrated CAF induction after siRNA mediated knockdown of PTEN in NHDFs. These CAFs showed similar marker gene expression and equivalent tumorigenic properties as described before.

Similar to our study, in hepatocellular carcinoma it was observed that the EV-mediated transfer of miR-21 into hepatic stellar cells resulted in suppression of PTEN and activation of the PI3K/AKT pathway, which ultimately led to the formation of CAFs (Zhou, Ren, et al. 2018).

A limitation of this study may be that at this point it did not analyse the relevance for EV-induced CAFs in promoting melanoma in vivo. In this context one would have to consider that other cells in the tumour microenvironment also secrete growth factors and cytokines which could generate CAFs and that injected fibroblasts may be transformed into CAFs rapidly by stimuli other than melanoma cell-derived EVs. One experimental design to show that EV-transported miR-92b-3p leads to the induction of tumour-promoting CAFs could encompass injection of melanoma cell derived EVs with and without miR-92b-3p knockout for 10–14 days, followed by injection of tumour cells, because this way one could assess the influence of miR-92b-3p on the priming of fibroblasts by melanoma cell-secreted EVs to form CAFs and their influence on promoting melanoma.

In conclusion, our study demonstrates that EVs, derived from melanoma cells, deliver miR-92b-3p into fibroblasts, which in turn induces CAF formation by targeting PTEN. We are elucidating a new mechanism by which melanoma cells induce CAF formation through intercellular communication via EVs

AUTHOR CONTRIBUTIONS

Stefanie Kewitz-Hempel: Data curation (equal); formal analysis (equal); investigation (equal); validation (equal); visualization (equal); writing—original draft (equal); writing—review and editing (equal). Nicola Windisch: Data curation (equal); investigation (equal). Gerd Hause: Methodology (equal). Lutz Müller: Conceptualization (equal); funding acquisition (equal). Cord Sunderkötter: Funding acquisition (equal); writing—original draft (equal); writing—review and editing (equal). Dennis Gerloff: Conceptualization (equal); formal analysis (equal); funding acquisition (equal); investigation (equal); project administration (equal); supervision (equal); visualization (equal); writing—original draft (equal); writing—review and editing (equal).

ACKNOWLEDGEMENTS

This study was supported by Wilhelm Roux Funding Program (FKZ 31/43) by the medical faculty of the Martin-Luther-University Halle-Wittenberg. We acknowledge the financial support within the funding program Open Access Publishing by the German Research Foundation (DFG). We would like to thank Anja Sobisch, Sylke Fasshauer, and Claudia Bruhne for excellent technical assistance.

CONFLICT OF INTEREST STATEMENT

The authors declare they have no conflict of interest.

ORCID

Stefanie Kewitz-Hempel  <https://orcid.org/0009-0009-4766-7025>

REFERENCES

- Ambros, V. (2004). The functions of animal microRNAs. *Nature*, 431, 350–355.
- Augsten, M. (2014). Cancer-associated fibroblasts as another polarized cell type of the tumor microenvironment. *Frontiers in Oncology*, 4, 62.
- Bardi, G. T., Smith, M. A., & Hood, J. L. (2018). Melanoma exosomes promote mixed M1 and M2 macrophage polarization. *Cytokine*, 105, 63–72.
- Bartel, D. P. (2004). MicroRNAs: Genomics, biogenesis, mechanism, and function. *Cell*, 116, 281–297.

- Bebelmann, M. P., Janssen, E., Pegtel, D. M., & Crudden, C. (2021). The forces driving cancer extracellular vesicle secretion. *Neoplasia*, *23*, 149–157.
- Biffi, G., & Tuveson, D. A. (2021). Diversity and biology of cancer-associated fibroblasts. *Physiological Reviews*, *101*, 147–176.
- Borges, F. T., Reis, L. A., & Schor, N. (2013). Extracellular vesicles: Structure, function, and potential clinical uses in renal diseases. *Brazilian Journal of Medical and Biological Research*, *46*, 824–830.
- Davidson, S., Efreanova, M., Riedel, A., Mahata, B., Pramanik, J., Huuhtanen, J., Kar, G., Vento-Tormo, R., Hagai, T., Chen, X., Haniffa, M. A., Shields, J. D., & Teichmann, S. A. (2020). Single-cell RNA sequencing reveals a dynamic stromal niche that supports tumor growth. *Cell Reports*, *31*, 107628.
- De Boeck, A., Hendrix, A., Maynard, D., Van Bockstal, M., Daniels, A., Pauwels, P., Gespach, C., Bracke, M., & De Wever, O. (2013). Differential secretome analysis of cancer-associated fibroblasts and bone marrow-derived precursors to identify microenvironmental regulators of colon cancer progression. *Proteomics*, *13*, 379–388.
- Dehne, N., Mora, J., Namgaladze, D., Weigert, A., & Brune, B. (2017). Cancer cell and macrophage cross-talk in the tumor microenvironment. *Current Opinion in Pharmacology*, *35*, 12–19.
- Dika, E., Broseghini, E., Porcellini, E., Lambertini, M., Riefolo, M., Durante, G., Loher, P., Roncarati, R., Bassi, C., Misciali, C., Negrini, M., Rigoutsos, I., Londin, E., Patrizi, A., & Ferracin, M. (2021). Unraveling the role of microRNA/isomiR network in multiple primary melanoma pathogenesis. *Cell Death & Disease*, *12*, 473.
- Doyle, L. M., & Wang, M. Z. (2019). Overview of extracellular vesicles, their origin, composition, purpose, and methods for exosome isolation and analysis. *Cells*, *8*, 727.
- Dror, S., Sander, L., Schwartz, H., Sheinboim, D., Barzilay, A., Dishon, Y., Apcher, S., Golan, T., Greenberger, S., Barshack, I., Malcov, H., Zilberberg, A., Levin, L., Nessling, M., Friedmann, Y., Igras, V., Barzilay, O., Vaknine, H., Brenner, R., & Levy, C. (2016). Melanoma miRNA trafficking controls tumour primary niche formation. *Nature Cell Biology*, *18*, 1006–1017.
- Erdogan, B., & Webb, D. J. (2017). Cancer-associated fibroblasts modulate growth factor signaling and extracellular matrix remodeling to regulate tumor metastasis. *Biochemical Society Transactions*, *45*, 229–236.
- Fang, T., Lv, H., Lv, G., Li, T., Wang, C., Han, Q., Yu, L., Su, B., Guo, L., Huang, S., Cao, D., Tang, L., Tang, S., Wu, M., Yang, W., & Wang, H. (2018). Tumor-derived exosomal miR-1247-3p induces cancer-associated fibroblast activation to foster lung metastasis of liver cancer. *Nature Communications*, *9*, 191.
- Flach, E. H., Rebecca, V. W., Herlyn, M., Smalley, K. S., & Anderson, A. R. (2011). Fibroblasts contribute to melanoma tumor growth and drug resistance. *Molecular Pharmacology*, *8*, 2039–2049.
- Friedrich, S., & Kraywinkel, K. (2018). Faktenblatt: Epidemiologie des malignen Melanoms in Deutschland. *Der Onkologe*, *24*, 447–452.
- Galbo, P. M., Zang, X. X., & Zheng, D. Y. (2021). Molecular features of cancer-associated fibroblast subtypes and their implication on cancer pathogenesis, prognosis, and immunotherapy resistance. *Clinical Cancer Research*, *27*, 2636–2647.
- Gerloff, D., Kewitz-Hempel, S., Hause, G., Ehrenreich, J., Golle, L., Kingreen, T., & Sunderkoetter, C. (2022). Comprehensive analyses of miRNAs revealed miR-92b-3p, miR-182-5p and miR-183-5p as potential novel biomarkers in melanoma-derived extracellular vesicles. *Frontiers in Oncology*, *12*, 935816.
- Gerloff, D., Lutzkendorf, J., Moritz, R. K. C., Wersig, T., Mader, K., Muller, L. P., & Sunderkotter, C. (2020). Melanoma-derived exosomal miR-125b-5p educates tumor associated macrophages (TAMs) by Targeting lysosomal acid lipase A (LIPA). *Cancers*, *12*(2), 464.
- Giusti, I., Di Francesco, M., Poppa, G., Esposito, L., D'Ascenzo, S., & Dolo, V. (2022). Tumor-derived extracellular vesicles activate normal human fibroblasts to a cancer-associated fibroblast-like phenotype, sustaining a pro-tumorigenic microenvironment. *Frontiers in Oncology*, *12*, 839880.
- Glabman, R. A., Choyke, P. L., & Sato, N. (2022). Cancer-associated fibroblasts: Tumorigenicity and targeting for cancer therapy. *Cancers*, *14*(16), 3906.
- Gong, L., Ren, M., Lv, Z., Yang, Y., & Wang, Z. (2018). miR-92b-3p promotes colorectal carcinoma cell proliferation, invasion, and migration by inhibiting FBXW7 in vitro and in vivo. *Dna and Cell Biology*, *37*, 501–511.
- Hanahan, D., & Coussens, L. M. (2012). Accessories to the crime: Functions of cells recruited to the tumor microenvironment. *Cancer Cell*, *21*, 309–322.
- Hu, T., & Hu, J. (2019). Melanoma-derived exosomes induce reprogramming fibroblasts into cancer-associated fibroblasts via Gm26809 delivery. *Cell Cycle*, *18*, 3085–3094.
- Kalluri, R. (2016). The biology and function of fibroblasts in cancer. *Nature Reviews Cancer*, *16*, 582–598.
- Kalluri, R., & Zeisberg, M. (2006). Fibroblasts in cancer. *Nature Reviews Cancer*, *6*, 392–401.
- Kanzaki, R., & Pietras, K. (2020). Heterogeneity of cancer-associated fibroblasts: Opportunities for precision medicine. *Cancer Science*, *111*, 2708–2717.
- Koyama, H., Kobayashi, N., Harada, M., Takeoka, M., Kawai, Y., Sano, K., Fujimori, M., Amano, J., Ohhashi, T., Kannagi, R., Kimata, K., Taniguchi, S., & Itano, N. (2008). Significance of tumor-associated stroma in promotion of intratumoral lymphangiogenesis: Pivotal role of a hyaluronan-rich tumor microenvironment. *American Journal of Pathology*, *172*, 179–193.
- Lange, T., Stracke, S., Rettig, R., Lendeckel, U., Kuhn, J., Schluter, R., Rippe, V., Endlich, K., & Endlich, N. (2017). Identification of miR-16 as an endogenous reference gene for the normalization of urinary exosomal miRNA expression data from CKD patients. *PLoS ONE*, *12*, E0183435.
- LeBleu, V. S., & Kalluri, R. (2018). A peek into cancer-associated fibroblasts: Origins, functions and translational impact. *Disease Models & Mechanisms*, *11*(4), dmm029447.
- Lei, L., Huang, Y., & Gong, W. (2014). Inhibition of miR-92b suppresses non-small cell lung cancer cells growth and motility by targeting RECK. *Molecular and Cellular Biochemistry*, *387*, 171–176.
- Li, C., Huo, B., Wang, Y., & Cheng, C. (2019). Downregulation of microRNA-92b-3p suppresses proliferation, migration, and invasion of gastric cancer SGC-7901 cells by targeting Homeobox D10. *Journal of Cellular Biochemistry*, *120*, 17405–17412.
- Li, M., Shan, W. L., Hua, Y., Chao, F. M., Cui, Y. Y., Lv, L., Dou, X. Y., Bian, X., Zou, J. L., Li, H., & Lin, W. C. (2021). Exosomal miR-92b-3p promotes chemoresistance of small cell lung cancer through the PTEN/AKT pathway. *Frontiers in Cell and Developmental Biology*, *9*, 661602.
- Livak, K. J., & Schmittgen, T. D. (2001). Analysis of relative gene expression data using real-time quantitative PCR and the 2^{-Delta Delta C(T)} method. *Methods (San Diego, California)*, *25*, 402–408.
- Marton, A., Vizler, C., Kusz, E., Temesfoi, V., Szathmary, Z., Nagy, K., Szegletes, Z., Varo, G., Siklos, L., Katona, R. L., Tubak, V., Howard, O. M., Duda, E., Minarovits, J., Nagy, K., & Buzas, K. (2012). Melanoma cell-derived exosomes alter macrophage and dendritic cell functions in vitro. *Immunology Letters*, *148*, 34–38.
- Mazurkiewicz, J., Simiczjzew, A., Dratkiewicz, E., Pietraszek-Gremplewicz, K., Majkowski, M., Kot, M., Zietek, M., Matkowski, R., & Nowak, D. (2022). Melanoma cells with diverse invasive potential differentially induce the activation of normal human fibroblasts. *Cell Communication and Signaling*, *20*(1), 63.
- Mir, B., & Goettsch, C. (2020). Extracellular vesicles as delivery vehicles of specific cellular cargo. *Cells*, *9*(7), 1601.
- Orimo, A., & Weinberg, R. A. (2007). Heterogeneity of stromal fibroblasts in tumors. *Cancer Biology & Therapy*, *6*, 618–619.

- Papaccio, F., Kovacs, D., Bellei, B., Caputo, S., Migliano, E., Cota, C., & Picardo, M. (2021). Profiling cancer-associated fibroblasts in melanoma. *International Journal of Molecular Sciences*, 22(14), 7255.
- Ping, Q., Yan, R., Cheng, X., Wang, W., Zhong, Y., Hou, Z., Shi, Y., Wang, C., & Li, R. (2021). Cancer-associated fibroblasts: Overview, progress, challenges, and directions. *Cancer Gene Therapy*, 28, 984–999.
- Raposo, G., & Stoorvogel, W. (2013). Extracellular vesicles: Exosomes, microvesicles, and friends. *Journal of Cell Biology*, 200, 373–383.
- Romano, V., Belviso, I., Venuta, A., Ruocco, M. R., Masone, S., Aliotta, F., Fiume, G., Montagnani, S., Avagliano, A., & Arcucci, A. (2021). Influence of tumor microenvironment and fibroblast population plasticity on melanoma growth, therapy resistance and immunoescape. *International Journal of Molecular Sciences*, 22(10), 5283.
- Schindelin, J., Arganda-Carreras, I., Frise, E., Kaynig, V., Longair, M., Pietzsch, T., Preibisch, S., Rueden, C., Saalfeld, S., Schmid, B., Tinevez, J. Y., White, D. J., Hartenstein, V., Eliceiri, K., Tomancak, P., & Cardona, A. (2012). Fiji: An open-source platform for biological-image analysis. *Nature Methods*, 9, 676–682.
- Shiga, K., Hara, M., Nagasaki, T., Sato, T., Takahashi, H., & Takeyama, H. (2015). Cancer-associated fibroblasts: Their characteristics and their roles in tumor growth. *Cancers (Basel)*, 7, 2443–2458.
- Shu, S., Yang, Y., Allen, C. L., Maguire, O., Minderman, H., Sen, A., Ciesielski, M. J., Collins, K. A., Bush, P. J., Singh, P., Wang, X., Morgan, M., Qu, J., Bankert, R. B., Whiteside, T. L., Wu, Y., & Ernstoff, M. S. (2018). Metabolic reprogramming of stromal fibroblasts by melanoma exosome microRNA favours a pre-metastatic microenvironment. *Scientific Reports*, 8, 12905.
- Strnadova, K., Pfeiferova, L., Prikryl, P., Dvorankova, B., Vlcek, E., Frydlova, J., Vokurka, M., Novotny, J., Sachova, J., Hradilova, M., Brabek, J., Smigova, J., Rosel, D., Smetana, K., Jr., Kolar, M., & Lacina, L. (2022). Exosomes produced by melanoma cells significantly influence the biological properties of normal and cancer-associated fibroblasts. *Histochemistry and Cell Biology*, 157, 153–172.
- Sunderkotter, C., Steinbrink, K., Goebeler, M., Bhardwaj, R., & Sorg, C. (1994). Macrophages and angiogenesis. *Journal of Leukocyte Biology*, 55, 410–422.
- Tang, S. L., Cheng, J. N., Yao, Y. F., Lou, C. J., Wang, L., Huang, X. Y., & Zhang, Y. Q. (2020). Combination of four serum exosomal miRNAs as novel diagnostic biomarkers for early-stage gastric cancer. *Frontiers in Genetics*, 11, 237.
- Tao, L., Huang, G., Song, H., Chen, Y., & Chen, L. (2017). Cancer associated fibroblasts: An essential role in the tumor microenvironment. *Oncology Letters*, 14, 2611–2620.
- Théry, C., Witwer, K. W., Aikawa, E., Alcaraz, M. J., Anderson, J. D., Andriantsitohaina, R., Antoniou, A., Arab, T., Archer, F., Atkin-Smith, G. K., Ayre, D. C., Bach, J. M., Bachurski, D., Baharvand, H., Balaj, L., Baldacchino, S., Bauer, N. N., Baxter, A. A., Bebawy, M., ... Zuba-Surma, E. K. (2018). Minimal information for studies of extracellular vesicles 2018 (MISEV2018): A position statement of the International Society for Extracellular Vesicles and update of the MISEV2014 guidelines. *Journal of Extracellular Vesicles*, 7(1), 1535750. <https://doi.org/10.1080/20013078.2018.1535750>
- Uotani, K., Fujiwara, T., Yoshida, A., Iwata, S., Morita, T., Kiyono, M., Yokoo, S., Kunisada, T., Takeda, K., Hasei, J., Numoto, K., Nezu, Y., Yonemoto, T., Ishii, T., Kawai, A., Ochiya, T., & Ozaki, T. (2017). Circulating microRNA-92b-3p as a novel biomarker for monitoring of synovial sarcoma. *Scientific Reports*, 7(1), 14634.
- Van Hove, L., & Hoste, E. (2022). Activation of fibroblasts in skin cancer. *Journal of Investigative Dermatology*, 142, 1026–1031.
- Villarroya-Beltri, C., Gutiérrez-Vázquez, C., Sánchez-Cabo, F., Pérez-Hernández, D., Vázquez, J., Martín-Cofreces, N., Martínez-Herrera, D. J., Pascual-Montano, A., Mittelbrunn, M., & Sánchez-Madrid, F. (2013). Sumoylated hnRNP2B1 controls the sorting of miRNAs into exosomes through binding to specific motifs. *Nature Communications*, 4, 2980.
- Vu, L. T., Peng, B., Zhang, D. X., Ma, V., Mathey-Andrews, C. A., Lam, C. K., Kiomourtzis, T., Jin, J., McReynolds, L., Huang, L., Grimson, A., Cho, W. C., Lieberman, J., & Le, M. T. (2019). Tumor-secreted extracellular vesicles promote the activation of cancer-associated fibroblasts via the transfer of microRNA-125b. *Journal of Extracellular Vesicles*, 8, 1599680.
- Wang, C., Uemura, M., Tomiyama, E., Matsushita, M., Koh, Y., Nakano, K., Hayashi, Y., Ishizuya, Y., Jingushi, K., Kato, T., Hatano, K., Kawashima, A., Ujike, T., Nagahara, A., Fujita, K., Imamura, R., Tsujikawa, K., & Nonomura, N. (2020). MicroRNA-92b-3p is a prognostic oncomiR that targets TSC1 in clear cell renal cell carcinoma. *Cancer Science*, 111, 1146–1155.
- Wang, C., Wang, Y., Chang, X., Ba, X., Hu, N., Liu, Q., Fang, L., & Wang, Z. (2020). Melanoma-derived exosomes endow fibroblasts with an invasive potential via miR-21 target signaling pathway. *Cancer Management Research*, 12, 12965–12974.
- Wang, G., Cheng, B., Jia, R. F., Tan, B., & Liu, W. L. (2021). Altered expression of microRNA-92b-3p predicts survival outcomes of patients with prostate cancer and functions as an oncogene in tumor progression. *Oncology Letters*, 21.
- Wang, W., Fu, S., Lin, X., Zheng, J., Pu, J., Gu, Y., Deng, W., Liu, Y., He, Z., Liang, W., & Wang, C. (2019). miR-92b-3p functions as a key gene in esophageal squamous cell cancer as determined by co-expression analysis. *Onco Targets and Therapy*, 12, 8339–8353.
- Whiteside, T. L. (2008). The tumor microenvironment and its role in promoting tumor growth. *Oncogene*, 27, 5904–5912.
- Wu, F., Yang, J., Liu, J., Wang, Y., Mu, J., Zeng, Q., Deng, S., & Zhou, H. (2021). Signaling pathways in cancer-associated fibroblasts and targeted therapy for cancer. *Signal Transduction and Targeted Therapy*, 6, 218.
- Xiao, D., Ohlendorf, J., Chen, Y., Taylor, D. D., Rai, S. N., Waigel, S., Zacharias, W., Hao, H., & McMasters, K. M. (2012). Identifying mRNA, microRNA and protein profiles of melanoma exosomes. *PLoS ONE*, 7, E46874.
- Xu, T., Wang, H., Jiang, M., Yan, Y., Li, W., Xu, H., Huang, Q., Lu, Y., & Chen, J. (2017). The E3 ubiquitin ligase CHIP/miR-92b/PTEN regulatory network contributes to tumorigenesis of glioblastoma. *American Journal of Cancer Research*, 7, 289–300.
- Yanez-Mo, M., Siljander, P. R., Andreu, Z., Zavec, A. B., Borrás, E. I., Buzas, E. I., Buzas, K., Casal, E., Cappello, F., Carvalho, J., Colas, E., Cordeiro-da Silva, A., Fais, S., Falcon-Perez, J. M., Ghobrial, I. M., Giebel, B., Gimona, M., Graner, M., & De Wever, O. (2015). Biological properties of extracellular vesicles and their physiological functions. *Journal of Extracellular Vesicles*, 4, 27066.
- Zaborowski, M. P., Balaj, L., Breakefield, X. O., & Lai, C. P. (2015). Extracellular vesicles: Composition, biological relevance, and methods of study. *Bioscience*, 65, 783–797.
- Zhou, L., Yang, K., Andl, T., Wickett, R. R., & Zhang, Y. (2015). Perspective of targeting cancer-associated fibroblasts in melanoma. *Journal of Cancer*, 6, 717–726.
- Zhou, X., Yan, T., Huang, C., Xu, Z., Wang, L., Jiang, E., Wang, H., Chen, Y., Liu, K., Shao, Z., & Shang, Z. (2018). Melanoma cell-secreted exosomal miR-155-5p induce proangiogenic switch of cancer-associated fibroblasts via SOCS1/JAK2/STAT3 signaling pathway. *Journal of Experimental & Clinical Cancer Research*, 37, 242.
- Zhou, Y., Ren, H., Dai, B., Li, J., Shang, L., Huang, J., & Shi, X. (2018). Hepatocellular carcinoma-derived exosomal miRNA-21 contributes to tumor progression by converting hepatocyte stellate cells to cancer-associated fibroblasts. *Journal of Experimental & Clinical Cancer Research*, 37, 324.

SUPPORTING INFORMATION

Additional supporting information can be found online in the Supporting Information section at the end of this article.

How to cite this article: Kewitz-Hempel, S., Windisch, N., Hause, G., Müller, L., Sunderkötter, C., & Gerloff, D. (2024). Extracellular vesicles derived from melanoma cells induce carcinoma-associated fibroblasts via miR-92b-3p mediated downregulation of PTEN. *Journal of Extracellular Vesicles*, 13, e12509. <https://doi.org/10.1002/jev2.12509>